

Relativistic effects on angular distribution and polarization of dielectronic satellite lines of hydrogenlike ions

M. H. Chen and J. H. Scofield

High Temperature Physics Division, Lawrence Livermore National Laboratory, Livermore, California 94550

(Received 3 April 1995)

The dielectronic satellite radiation emitted from ions excited by resonant capture of an electron from a directed electron beam can be strongly linearly polarized. We have carried out relativistic calculations of angular asymmetry parameters and polarization of dielectronic satellite lines for H-like ions with $Z = 9, 22, 28, 42,$ and 92 using the multiconfiguration Dirac-Fock model. We found that many transitions exhibit strong angular asymmetry and a large degree of polarization. In addition, we found that the polarization of the resulting radiation is independent of atomic number in the nonrelativistic limit. But when the effects of relativity are taken into account, the polarization becomes markedly Z dependent.

PACS number(s): 34.80.Kw

I. INTRODUCTION

In a plasma the radiation emitted following electron collisional excitation, ionization, or resonant dielectronic capture can be polarized when the electron distribution is anisotropic. This occurs in some astrophysical plasmas [1] as well as in laboratory-produced plasmas under conditions in which the ions are excited by a directed electron beam [2]. Under these circumstances, the magnetic sublevels of the excited states may not be populated statistically. The degree of polarization depends on the extent of deviation from the statistical populations of the excited magnetic sublevels of the ions.

Recently, the effects of relativity have been found to exert strong influence on the polarization of radiation emitted from ions excited by a directed electron beam [3]. The polarization was found to be markedly dependent on atomic number Z instead of Z independent as predicted by nonrelativistic theory [4]. In addition, relativistic effects have also been found to be very important in the calculations of angular distribution parameters for the Auger electrons following electron impact excitation [5]. Inal and Dubau have carried out the formulation of the linear polarization of dielectronic satellite lines, using density-matrix formalism [6], and applied it to He-like Fe^{24+} . In this paper, we present the results of our investigation of relativistic effects on the angular distribution and polarization of dielectronic recombination (DR) satellite lines of hydrogenlike ions. We calculated the angular distribution and polarization of DR satellite lines of H-like ions with $Z = 9, 22, 28, 42,$ and 92 , using the relativistic multiconfiguration Dirac-Fock (MCDF) model, and then repeated the calculations in the nonrelativistic limit.

II. THEORETICAL METHOD

In our present work, dielectronic recombination is treated as a two-step process: dielectronic capture followed by radiative stabilization. The effects of overlapping resonances and interference between the direct radiative recombination and dielectronic recombination are

neglected. The dielectronic capture probability can be calculated as an inverse Auger transition by detail balance. The angular distribution of Auger electrons has been presented in Ref. [7]. Briefly, the dielectronic recombination probability can be written as

$$T(i \rightarrow f) = \frac{A_{\text{cap}}(i \rightarrow d) A_r(d \rightarrow f)}{\sum_j A_A(d \rightarrow j) + \sum_k A_r(d \rightarrow k)}. \quad (1)$$

Here, $A_r(d \rightarrow f)$ is the radiative rate, and $A_A(d \rightarrow j)$ is the Auger rate. The capture probability A_{cap} after averaging over the electron spin and initial magnetic substates is given by

$$\begin{aligned} A_{\text{cap}}(i \rightarrow d) &= \frac{1}{2(2J_i + 1)} \sum_{M_i, m_s} \frac{2\pi}{\hbar} \left| \langle \Psi_{J_d M_d} | V | \Psi_{J_i M_i} \Phi_{E k m_s}^{(+)} \rangle \right|^2, \\ &= \frac{2J_d + 1}{2(2J_i + 1)} A_A(d \rightarrow i), \end{aligned} \quad (2)$$

where Ψ_{J_i} and Ψ_{J_d} are the antisymmetrized many-electron wave functions for the initial and autoionizing states, respectively, and V is the two-electron interaction operator. The incoming free electron with definite energy E , momentum \mathbf{p} , and spin can be expressed as superpositions of partial waves [8]

$$\Phi_{E k m_s}^{(+)} = \sum_{\kappa, m} i^l e^{i\delta_\kappa} \Omega_{\kappa m}^{(+)}(\hat{\mathbf{p}}) \chi_{l/2 m_s} \psi_{\kappa m}(r), \quad (3)$$

with

$$\Omega_{\kappa m} = \sum_{m_1, \mu} Y_{lm_1}(\theta, \varphi) \chi_{l/2 \mu} \langle l m_1 1/2 \mu | l 1/2 j m \rangle. \quad (4)$$

Here, $\psi_{\kappa m}$ is the one-electron Dirac orbital, $\kappa = (l - j)(2j + 1)$ is the relativistic quantum number, l and j are the orbital and total angular momentum of the continuum electron, and δ_κ is the phase shift. The spontaneous radiative transition rate is calculated from the perturbation theory by using the multipole expansion [9,10]

$$A_r(d \rightarrow f) = 2\pi \sum_{L,q} \left| (-1)^{J_f - M_f} \begin{Bmatrix} J_f & L & J_d \\ -M_f & q & M_d \end{Bmatrix} \langle J_f \| (\vec{\alpha} \cdot \vec{A})^L \| J_d \rangle \right|^2. \quad (5)$$

After some algebra, the energy-averaged differential cross section from an initial state i to a final state f via an intermediate state d is given by [11–13]

$$\frac{d\bar{\sigma}(idf)}{d\Omega} = \frac{\bar{\sigma}(idf)}{4\pi} W(\theta), \quad (6)$$

where the total DR cross section $\bar{\sigma}(idf)$ can be expressed in atomic units as [12]

$$\bar{\sigma}(idf) = \frac{\pi^2 g_d}{2\Delta E E_d g_i} \frac{A_A(d \rightarrow i) A_r(d \rightarrow f)}{\sum_j A_A(d \rightarrow j) + \sum_k A_r(d \rightarrow k)}. \quad (7)$$

Here, $g_d = 2J_d + 1$ and $g_i = 2J_i + 1$ are the statistical weight factors for the intermediate and initial states, respectively; E_d is the Auger energy; and ΔE is the energy bin. For the electric-dipole ($E1$) transition, the angular distribution $W(\theta)$ averaged over the polarization is given by [11]

$$W(\theta) = 1 + \beta P_2(\cos\theta), \quad (8)$$

with the anisotropy parameter

$$\beta = (-1)^{1+J_d+J_f} \left[\frac{3(2J_d+1)}{2} \right]^{1/2} \begin{Bmatrix} 1 & 1 & 2 \\ J_d & J_d & J_f \end{Bmatrix} \frac{P_{J_i J_d}^{(2)}}{P_{J_i J_d}^{(0)}}, \quad (9)$$

and

$$P_{J_i J_d}^{(L)} = \frac{1}{2(2J_i+1)} \left[\sum_{\kappa, \kappa'} (-1)^{J_i+L+J_d-1/2} (i)^{l-l'} \cos(\delta_\kappa - \delta_{\kappa'}) [j, j', l, l', L]^{1/2} \right. \\ \left. \times \begin{Bmatrix} l & l' & L \\ 0 & 0 & 0 \end{Bmatrix} \begin{Bmatrix} j' & j & L \\ l & l' & \frac{1}{2} \end{Bmatrix} \begin{Bmatrix} J_d & J_d & L \\ j & j' & J_i \end{Bmatrix} \langle J_d \| V \| J_i j J_d \rangle \langle J_d \| V \| J_i j' J_d \rangle^* \right]. \quad (10)$$

Here, J_i , J_d , and J_f are the total angular momenta for the initial ionic state, intermediate autoionizing, and stabilized x-ray final states, respectively; $P_2(\cos\theta) = \frac{1}{2}(3\cos^2\theta - 1)$, where θ is the angle of emission of x-ray with respect to the beam axis; $[a, b, \dots] = [(2a+1), (2b+1), \dots]$ and $\langle J_d \| V \| J_i j J_d \rangle$ is the reduced Auger matrix element.

The degree of linear polarization can be defined as [11]

$$P(\theta) = \frac{I_{\parallel} - I_{\perp}}{I_{\parallel} + I_{\perp}}, \quad (11)$$

where $I_{\parallel}(I_{\perp})$ is the intensity of the emitted photons with polarization vector parallel (perpendicular) to the meridian plane (i.e., the plane formed by the directions of the incident beam and of the detection of radiation). The polarization fraction is related to the asymmetry parameter by [11,14]

$$P(\theta) = \frac{3\beta \sin^2\theta}{\beta(1-3\cos^2\theta)-2}. \quad (12)$$

The atomic transition rates required in the present work are calculated from the perturbation theory, using the MCDF model [9,15]. In the MCDF model, the single-particle central-field Dirac orbital is chosen as [15]

$$\psi_{n\kappa m}(\mathbf{r}) = \frac{1}{r} \begin{bmatrix} P_{n\kappa}(r)\Omega_{\kappa m} \\ iQ_{n\kappa}(r)\Omega_{-\kappa m} \end{bmatrix}. \quad (13)$$

Here, $P_{n\kappa}(r)$ and $Q_{n\kappa}(r)$ are the large and small components of the radial wave functions, respectively; $\Omega_{\kappa m}$ is the j - j coupled wave function of the angular momentum and spin as defined in Eq. (4). An atomic-state function for a state i with total angular momentum JM is constructed from the configuration state functions (CSF's):

$$\Psi_i(JM) = \sum_{\lambda=1}^n C_{i\lambda} \phi(\Gamma_{\lambda} JM), \quad (14)$$

where n is the number of CSF's included in the expansion and $C_{i\lambda}$ are the mixing coefficients, which are determined by diagonalizing the energy matrix. The CSF's are formed by taking a linear combination of the Slater determinants constructed from the Dirac orbitals.

The Auger transition rate is calculated in the frozen-orbital approximation [9,13], with the two-electron operator $V_{\alpha\beta}$ in Eq. (2) taken to be the sum of Coulomb and generalized Breit operators [15,16]. The radiative $E1$ transition rates are calculated from perturbation theory according to Eq. (5).

III. NUMERICAL CALCULATIONS

The K - LL DR process from the H-like ground state to He-like ions can be described schematically by

$$e + 1s \rightarrow 2l2l' \rightarrow 1s2l'' + h\nu. \quad (15)$$

The energies and wave functions for the bound states

TABLE I. Angular anisotropy parameter β for the hydrogenlike dielectronic recombination satellite lines.

| Transition | F ⁷⁺ | Ti ²⁰⁺ | Ni ²⁶⁺ | Mo ⁴⁰⁺ | U ⁹⁰⁺ |
|---------------------------|-----------------|-------------------|-------------------|-------------------|------------------|
| $2s2p\ ^3P_1-1s2s\ ^3S_1$ | -0.249 | -0.105 | 0.067 | 0.125 | -0.111 |
| $2s2p\ ^3P_1-1s2s\ ^1S_0$ | 0.497 | 0.209 | -0.133 | -0.249 | 0.221 |
| $2s2p\ ^3P_2-1s2s\ ^3S_1$ | -0.350 | -0.350 | -0.350 | -0.343 | -0.334 |
| $2p^2\ ^3P_1-1s2p\ ^3P_0$ | -0.195 | -0.173 | -0.165 | -0.271 | -0.159 |
| $2p^2\ ^3P_1-1s2p\ ^3P_1$ | 0.097 | 0.086 | 0.083 | 0.136 | 0.080 |
| $2p^2\ ^3P_1-1s2p\ ^3P_2$ | -0.020 | -0.017 | -0.017 | -0.027 | -0.016 |
| $2p^2\ ^3P_1-1s2p\ ^1P_1$ | 0.097 | 0.086 | 0.083 | 0.136 | 0.080 |
| $2p^2\ ^3P_2-1s2p\ ^3P_1$ | -0.500 | -0.500 | -0.500 | -0.500 | -0.499 |
| $2p^2\ ^3P_2-1s2p\ ^3P_2$ | 0.500 | 0.500 | 0.500 | 0.500 | 0.499 |
| $2p^2\ ^3P_2-1s2p\ ^1P_1$ | -0.500 | -0.500 | -0.500 | -0.500 | -0.499 |
| $2p^2\ ^1D_2-1s2p\ ^3P_1$ | -0.500 | -0.500 | -0.500 | -0.499 | -0.462 |
| $2p^2\ ^1D_2-1s2p\ ^3P_2$ | 0.500 | 0.500 | 0.500 | 0.499 | 0.462 |
| $2p^2\ ^1D_2-1s2p\ ^1P_1$ | -0.500 | -0.500 | -0.500 | -0.499 | -0.462 |
| $2s2p\ ^1P_1-1s2s\ ^3S_1$ | 0.500 | 0.499 | 0.498 | 0.477 | 0.338 |
| $2s2p\ ^1P_1-1s2s\ ^1S_0$ | -1.000 | -0.999 | -0.996 | -0.954 | -0.677 |

were computed by using the MCDF model with an average-level scheme [15] in intermediate coupling with configuration interaction from the same complex. The continuum wave functions were generated by solving the Dirac-Fock equations in the final-state potential. The phase shifts in Eq. (10) were determined according to a procedure given by Zhang, Sampson, and Clark [17]. These reduced Auger matrix elements and phase shifts were then employed to calculate the asymmetry parameter β according to Eqs. (9) and (10). The linear polarization fractions were evaluated according to Eq. (12). The corresponding nonrelativistic values were obtained by repeating the calculations with velocity of light increased a thousandfold to simulate the nonrelativistic limit.

IV. RESULTS AND DISCUSSION

We have carried out a systematic study of relativistic effects on the angular distribution and polarization of the dielectronic satellite lines of H-like ions. The effects of relativity on the Auger matrix elements can arise from changes in the energy, from shifts in wave functions, and from the Breit interaction. The net effect depends on the strengths and phases of each component and cannot be easily predicted. The changes in Auger matrix elements due to relativity will affect the population density $P_{J_i J_d}^{(L)}$ and the anisotropy parameter β . The angular anisotropy parameters β for the hydrogenlike DR satellite lines with $Z = 9, 22, 28, 42,$ and 92 are listed in Table I. The asymmetry parameters are quite large, ranging from -1 to 0.5 . For the transitions originating from the $2p^2\ ^3P_2$ and 1D_2 states, the β parameters are nearly independent of atomic number and all have the same absolute value of 0.5 . This is due to the fact that the transitions $2p^2\ J=2 \rightarrow 1s2p\ J=1,2$ have the same values for the $6-j$ symbol in Eq. (9). In addition, the alignment parameter due to resonant electron capture $P_{J_i J_d}^{(2)}/P_{J_i J_d}^{(0)}$ is independent of Z in the nonrelativistic limit, since only one partial wave ϵd is allowed. On the other hand, the β values display strong Z dependency for transitions involving the $2s2p\ ^3P_1$ initial state. We included only electric-dipole

radiation in the present work. Higher multipoles contribute very little to the total radiative rate. For example, they contribute less than 1% even for an ion as heavy as U⁹⁰⁺.

In Figs. 1–4, the angular distribution functions $W(\theta)$ and linear polarization $P(\theta)$ for the $2s2p\ ^3P_1-1s2s\ ^3S_1$, $2s2p\ ^3P_1-1s2s\ ^1S_0$, $2s2p\ ^1P_1-1s2s\ ^1S_0$, and $2p^2\ ^1D_2-1s2p\ ^1P_1$ transitions in F⁷⁺, Mo⁴⁰⁺, and U⁹⁰⁺ are shown. From these comparisons, the following observations can

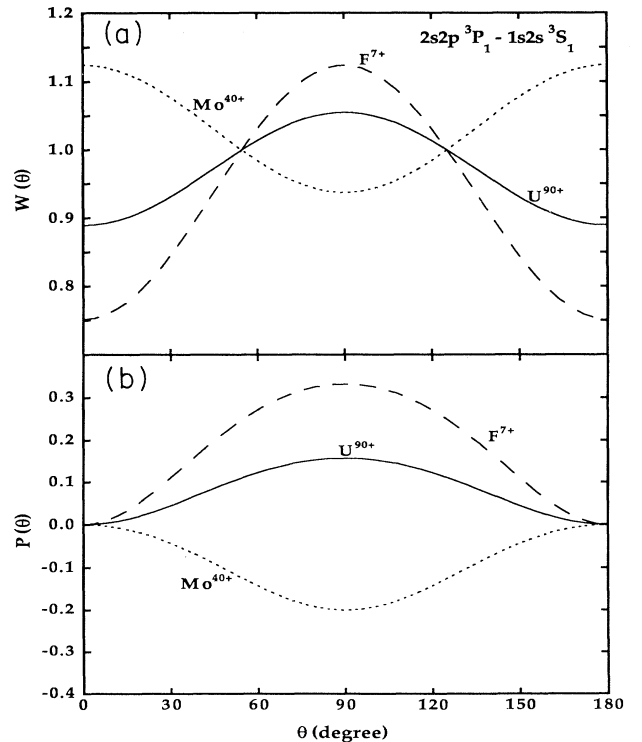


FIG. 1. Angular distribution function $W(\theta)$ and polarization $P(\theta)$ for the $2s2p\ ^3P_1-1s2s\ ^3S_1$ transition as functions of θ . $W(\theta)$ and $P(\theta)$ are displayed in (a) and (b), respectively.

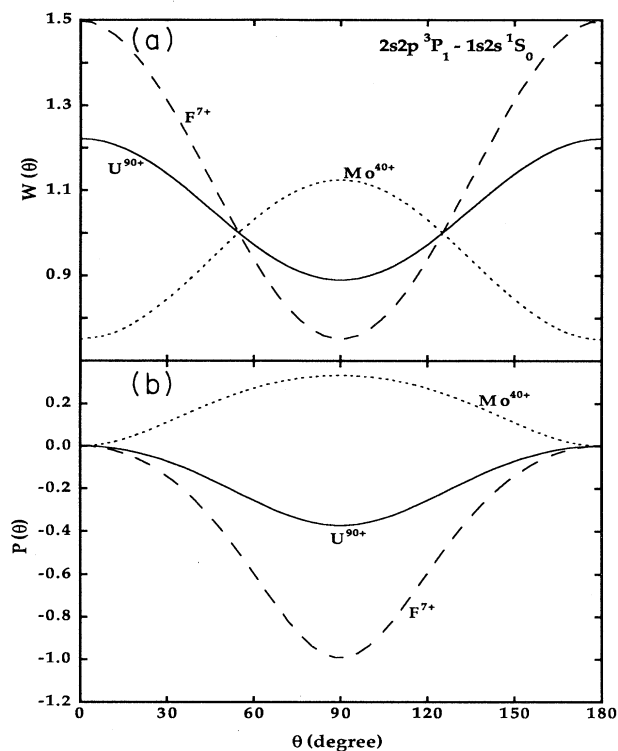


FIG. 2. Angular distribution and polarization for the $2s2p\ ^3P_1 - 1s2s\ ^1S_0$ transition as functions of θ .

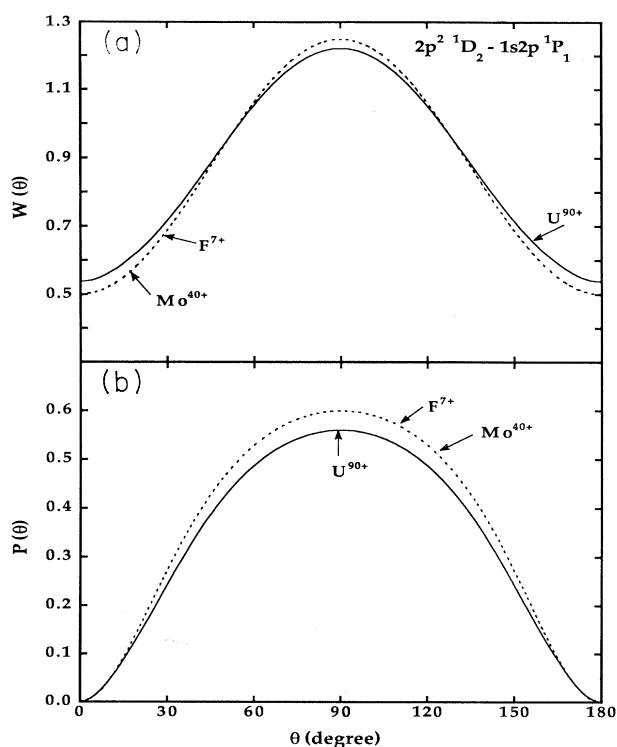


FIG. 4. Angular distribution and polarization for the $2p^2\ ^1D_2 - 1s2p\ ^1P_1$ transition.

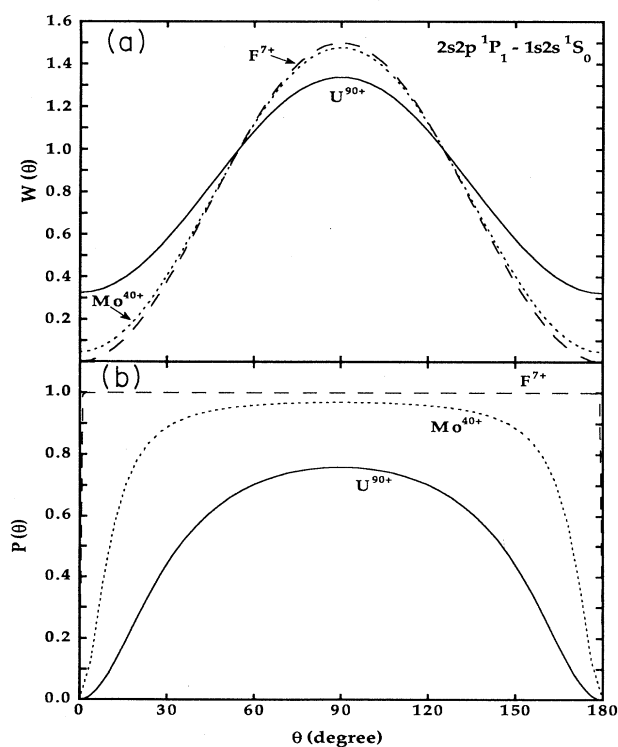


FIG. 3. Angular distribution and polarization for the $2s2p\ ^1P_1 - 1s2s\ ^1S_0$ transition.

be made. (i) For many transitions, the DR satellite lines exhibit strong angular asymmetry and a large degree of polarization. (ii) Strong Z dependency can be seen for transitions arising from the $2s2p$ initial states but not from the $2p^2\ ^1D_2$ state. (iii) Effects of relativity tend to reduce the angular asymmetry and the degree of polarization. (iv) For the $2s2p\ ^1P_1 - 1s2s\ ^1S_0$ transition, the β value is nearly equal to -1 for low- Z ions. This DR line shows 100% polarization for all angles except those near 0° and 180° for F^{7+} [Fig. 3(b)]. The change of β value from -1 to -0.677 from $Z=9$ to 92 (see Table I) due to effects of relativity drastically alters the behavior of polarization as a function of θ . At $\theta=30^\circ$ the relativistic effects reduce the polarization fraction from 100% to 40% as Z increases from 9 to 92.

In Figs. 5 and 6, the polarization fractions at $\theta=90^\circ$ for the $2s2p\ ^1P_1 - 1s2s\ ^1S_0$, $2s2p\ ^3P_1 - 1s2s\ ^3S_1$, and $2s2p\ ^3P_1 - 1s2s\ ^1S_0$ transitions from nonrelativistic and relativistic calculations are compared. One can see that the nonrelativistic results are independent of Z , while the relativistic values show strong Z dependence. For the $2s2p\ ^1P_1 - 1s2s\ ^1S_0$ transition, effects of relativity reduce the polarization fraction by 25% at $Z=92$. For the $2s2p\ ^3P_1 - 1s2s\ ^3S_1$ transition, the relativistic effects change the degree of polarization from 0.35 to -0.25 at $Z=42$.

In summary, we have calculated the angular distribution and polarization of DR satellite lines for F^{7+} , Ti^{20+} , Ni^{26+} , Mo^{40+} , and U^{90+} . We found that many transitions show strong angular asymmetry and polarization.

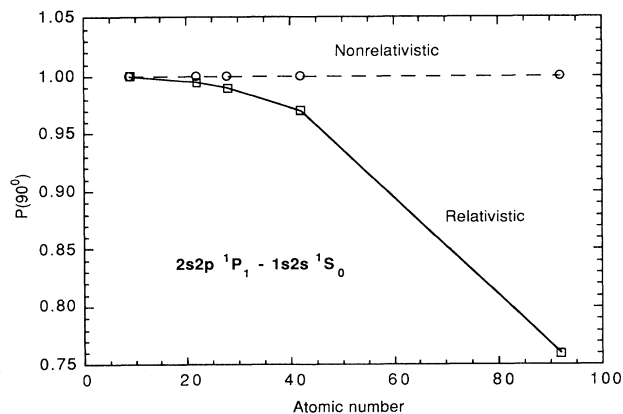


FIG. 5. The degree of polarization at $\theta=90^\circ$ for the $2s2p\ ^1P_1 - 1s2s\ ^1S_0$ transition as functions of atomic number. The broken curve indicates the nonrelativistic values. The solid curve displays the relativistic results.

We also found that the degree of polarization from non-relativistic calculations are independent of Z . However, the polarization fractions become markedly Z dependent when the effects of relativity are included in the calculations.

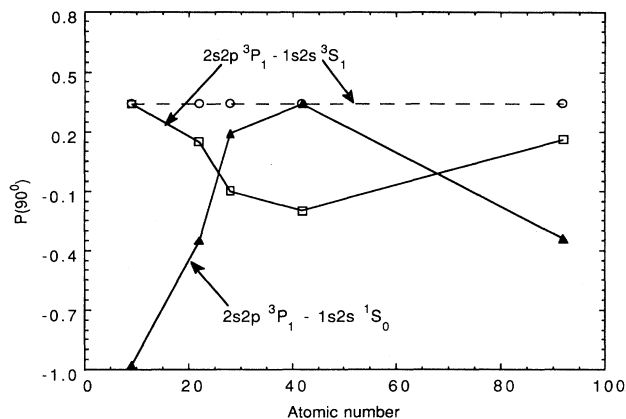


FIG. 6. The polarization fractions at $\theta=90^\circ$ for the $2s2p\ ^3P_1 - 1s2s\ ^3S_1, ^1S_0$ transitions. The symbols are the same as in Fig. 5.

ACKNOWLEDGMENTS

This work was performed under the auspices of the U.S. Department of Energy by Lawrence Livermore National Laboratory under Contract No. W-7405-Eng-48.

-
- [1] E. Haug, *Sol. Phys.* **71**, 77 (1981).
 [2] E. Källne and J. Källne, *Phys. Scr.* **T17**, 152 (1987).
 [3] K. J. Reed and M. H. Chen, *Phys. Rev. A* **48**, 3644 (1993).
 [4] Y. Itkawa, R. Srivastava, and K. Sakimoto, *Phys. Rev. A* **44**, 7195 (1991).
 [5] M. H. Chen and K. J. Reed, *Phys. Rev. A* **50**, 2279 (1994).
 [6] M. K. Inal and J. Dubau, *J. Phys. B* **22**, 3329 (1989); **20**, 4221 (1987).
 [7] M. H. Chen, *Phys. Rev. A* **45**, 1684 (1992).
 [8] R. H. Pratt, A. Ron, and H. K. Tseng, *Rev. Mod. Phys.* **45**, 273 (1973).
 [9] M. H. Chen, *Phys. Rev. A* **31**, 1449 (1985).
 [10] I. P. Grant, *J. Phys. B* **7**, 1458 (1974).
 [11] I. C. Percival and M. J. Seaton, *Philos. Trans. R. Soc. London, Ser. A* **251**, 113 (1958).
 [12] K. LaGattuta and Y. Hahn, *Phys. Rev. A* **24**, 2273 (1981); *J. Phys. B* **15**, 2101 (1982).
 [13] M. H. Chen, in *Recombination of Atomic Ions*, Vol. 296 of *NATO ASI Series B: Physics*, edited by W. G. Graham, W. Fritsch, Y. Hahn, and J. A. Tanis (Plenum, New York, 1992), p. 61.
 [14] N. R. Badnell, *Phys. Rev. A* **42**, 3795 (1990).
 [15] I. P. Grant *et al.*, *Comput. Phys. Commun.* **21**, 207 (1980).
 [16] W. R. Johnson and K. T. Cheng, in *Atomic Inner-shell Physics*, edited by B. Crasemann (Plenum, New York, 1985), p. 3.
 [17] H. L. Zhang, D. H. Sampson, and R. E. H. Clark, *Phys. Rev. A* **41**, 198 (1990).